

High mobility in ZnO thin films deposited on perovskite substrates with a low temperature nucleation layer

E. Bellingeri,^{a)} D. Marré, I. Pallecchi, L. Pellegrino, and A. S. Siri

INFN-Lamia, Corso Perrone 24, 16152 Genova, Italy and Dipartimento di Fisica, Università di Genova, Via Dodecaneso 33, 16146 Genova, Italy

(Received 11 August 2004; accepted 2 November 2004; published online 27 December 2004)

High electron mobility is measured down to low temperature in epitaxial ZnO thin films deposited on (110) oriented strontium titanate substrates. Electron mobility is evaluated by both magnetoresistance and resistivity-Hall effect data. Values up to $400 \text{ cm}^2/\text{V s}$ are found below 50 K in epitaxial thin films grown by a two-step method: first a 100-nm-thick ZnO relaxing layer is deposited on the SrTiO_3 (110) substrate at relatively low temperature (550–600 °C) and then the deposition temperature is raised up to 800 °C for the growth of a second ZnO layer. Reflection high energy electron diffraction analysis during the deposition, *ex situ* x-ray diffraction and AFM morphology studies performed separately on each layer reveal that the first layer grows in a quasi-two-dimensional mode while the increased temperature in the second step improves the crystalline quality of the film. The integration of ZnO transparent semiconductor with high- k dielectric perovskite substrates may lead to a wide variety of new electronic/optoelectronic devices. © 2005 American Institute of Physics. [DOI: 10.1063/1.1844034]

High quality zinc oxide thin films are of tremendous interest for applications in electronic and optoelectronic¹ devices, ZnO being a transparent semiconductor with a tunable energy gap around 3.2 eV and showing large piezoelectric parameters. Recently, due to its high electron mobility values compared to other oxide semiconductors, it has been employed as a semiconducting channel in transistor devices² like ZnO– SiO_2 –Si heterostructures.^{3,4}

Usually, ZnO epitaxial growth is obtained depositing on Al_2O_3 (Refs. 5 and 6) or Si (Ref. 7) substrates whose hexagonal structure matches the ZnO lattice. However, lattice mismatch between ZnO and these substrates strains the structure and structural and transport properties similar to single crystals have been obtained only for thick films.⁸ Recently, a buffer layer of ZnO, deposited at relatively low temperature, has been introduced to relax lattice strain and improve carrier mobility.^{9,10} Using this relaxation layer, values up to $150 \text{ cm}^2/\text{V s}$ at room temperature have been measured for samples thinner than 1 μm .

In this work we present our study on the compatibility of ZnO with a perovskite-type crystal structure that has a pseudocubic cell.^{11,12}

Perovskites are extensively studied for their wide spectrum of physical properties. Many examples of prototype electronic devices based on the exotic properties of perovskite oxides already exist, exploiting phenomena such as superconductivity, ferroelectricity, ferromagnetism, antiferromagnetism, charge and spin orderings, colossal magnetoresistance, and metal–insulator transition.^{13–17} Within this scenario, new possibilities can be envisaged for ZnO-based devices if ZnO is integrated in perovskite heterostructures.

Thin ZnO films (thicknesses ranging from 20 to 1000 nm) are deposited by pulsed laser ablation from a sintered commercial ZnO target (99.999% pure) on strontium titanate substrates with different crystal orientations. The growth is carried on under a wide range of deposition conditions: tem-

peratures from 550 to 800 °C, oxygen pressures from 10^{-5} to $2 \cdot 10^{-2}$ mbar. For the experiment reported here, laser fluency, laser frequency, and target–substrate distance are kept constant at $2 \text{ J}/\text{cm}^2$, 3 Hz, and 48 mm, respectively. Structural and morphological properties of the samples are investigated *in situ* by reflection high energy electron diffraction (RHEED) analysis and *ex situ* by x-ray diffraction using a four-circle diffractometer, scanning electron microscopy, and atomic force microscopy. ZnO grows textured both on (100) and (110) oriented substrates, but whereas in the first case the ZnO 101 crystal axis is perpendicular to the surface and two in-plane orientations are present, *c*-axis oriented ZnO epitaxial films are obtained on (110) STO substrates. All the experiments reported in the following are referred to samples deposited on (110) STO substrates.

For these samples, epitaxial growth is found in the whole range of deposition parameters. An example of ϕ scans of STO 100 and ZnO 101 reflections are reported in Fig. 1 showing that ZnO grows with the side of the hexagon parallel to the short side of the rectangular surface cell of STO 110. The growth in this orientation is driven by the good matching of the long side of the rectangle of STO ($a_{\text{STO}}\sqrt{2} = 5.515 \text{ \AA}$) with the ZnO hexagon apothem ($a_{\text{ZnO}}\sqrt{3}$

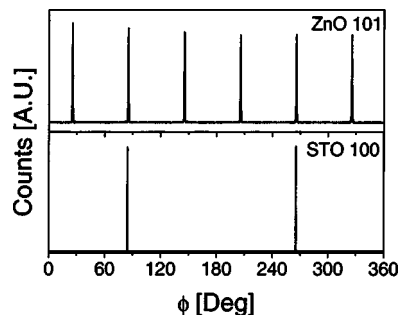


FIG. 1. ϕ scans of the ZnO101 and STO 100 reflections: ZnO grows with the side of the hexagon parallel to the short side of the rectangular surface cell of STO 110.

^{a)}Electronic mail: bellingeri@fisica.unige.it

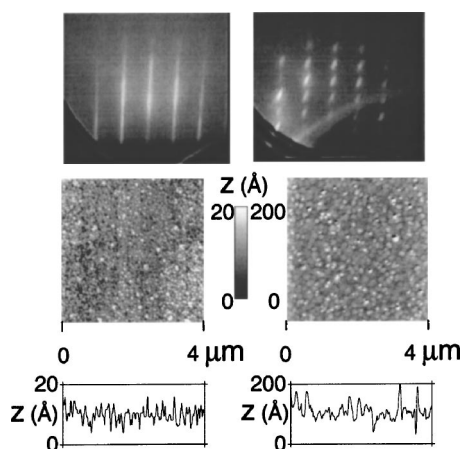


FIG. 2. RHEED and AFM images of ZnO thin films grown at 570 °C (left) and 800 °C (right); The rms roughness of the two films are 0.43 and 2.9 nm, respectively. By lowering the deposition temperature a quasi-two-dimensional growth mode can be achieved.

$=5.611 \text{ \AA}$), the resulting mismatch being lower than 2%. In the perpendicular direction, a higher order matching with a mismatch of 1.5% can also be found for six ZnO over five STO cells. Nevertheless we regard the lower order matching as the leading mechanism of the growth in agreement to what was reported in Ref. 18 where a uniaxial locked epitaxy results in high crystalline quality ZnO thin films.

Concerning the out-of-plane orientation, rocking curve widths [full width at half maximum (FWHM)] from 0.4° down to 0.18° are measured, with the FWHM decreasing as the thickness increases.⁸

Whereas single-phase ZnO films are obtained from 550 to 800 °C, the substrate temperature is found to be a key parameter for the growth mode and for the morphological properties of the film surface. As clearly shown in RHEED images reported in Fig. 2, the growth is quasi-two-dimensional at low temperature whereas it assumes a pronounced transmission (three-dimensional) character at high temperature. This behavior is observed not only at the end of the growth but since the earliest stages of the growth: we think that this effect is related to a low chemical affinity between the ZnO and the substrate and the high mobility of the atomic species on the surface, leading to a preferential island and columnar growth. At low temperature the surface mobility is depressed thus resulting in a more uniform coverage.

AFM measurements are in agreement with the RHEED observations. The films deposited at low temperature (570 °C) have very smooth surfaces and very low roughness (below 0.5 nm rms) whereas rms roughness around 3 nm is found for films deposited at 800 °C. In Fig. 2 the RHEED patterns of two 100-nm-thick films grown at 570 and 800 °C are shown together with the morphological analysis of their surfaces.

The thicknesses as well as the optical spectra of ZnO thin films are obtained by spectroscopic ellipsometry¹⁹ using a M-2000S™ variable angle Fast Spectroscopic Ellipsometer and a W-VASE software data analysis system both from J. A. Woollam Co., Inc. Measurements are carried out in air in the energy range 1.71–5.05 eV. Data analysis is performed taking into account the effects of surface roughness measured by atomic force microscopy and introducing a three-layer model (substrate/film/surface roughness). The optical con-

stants of the STO substrate and the ZnO film are modeled by using the Herzinger–Johs parametrization,^{20,21} while the (variable thickness) surface roughness layer is introduced in the framework of the effective medium approximation^{21,22} where a mixture (50-50%) of ZnO and voids is assumed. The optical properties of our films reveal characteristics similar to those found in literature for pure ZnO,^{23,24} presenting no absorption in the visible part of the spectrum and a band gap of about 3.3 eV.

Epitaxial ZnO thin films show good structural, morphological, and optical properties, but poor transport properties are measured. All the samples show semiconducting behavior of the resistivity regardless of their carrier concentration, which is in the range from 10^{16} to 10^{19} e/cm^3 , depending on the oxygen deposition pressure. The carrier mobility at room temperature never exceeds $15 \text{ cm}^2/\text{V s}$ and decreases when lowering the temperature. Such low mobility values are expected in the large carrier concentration region^{25,26} (above $5 \times 10^{17} \text{ e/cm}^3$), where it can be ascribed to impurities scattering, electronic correlation mechanisms, and scattering from defects, whereas we do not observe an increase in the mobility of lightly doped samples^{9,27} probably because of structural disorder.

In particular, it seems to be a quite difficult task to obtain ZnO films with low structural disorder in the range of deposition temperature that we explored. At high deposition temperature, indeed, the crystalline quality of single grains of the film improves but granularity due to the columnar growth mode is a limiting factor for the carrier mobility; at low deposition temperature, instead, the film grows in a more uniform way but due to the lattice mismatch, a larger residual strain is present in the ZnO structure favoring defect formation; thereby the mobility is depressed both due to the strain effects and to the large number of carriers created by the disorder.¹⁰

To overcome this problem, starting from these observations and following Refs. 9 and 10, the deposition is carried out in two steps: at first a relatively thin ZnO layer (50-100 nm thick) is grown at low temperature (550–600 °C) in such a way as to obtain a uniform coverage of the substrate, thus realizing a relaxation layer; then the temperature is raised up to 750 °C and a thicker layer with high crystalline quality is deposited. AFM images and SEM investigations show that the low temperature relaxation layer is highly effective in suppressing the columnar growth, allowing one to obtain homogeneous and well-connected samples. With the mobility maximum foreseen for a carrier concentration of the order of 10^{17} e/cm^3 ,^{9,27} we choose an oxygen deposition pressure of $7 \times 10^{-3} \text{ mbar}$ on the basis of an optimization process carried out on the single thin layer films.

The drop of the disorder due to the introduction of the buffer layer is clearly observable in the transport properties of the films. In samples with carrier concentrations as low as $5\text{--}7 \times 10^{16} \text{ e/cm}^3$ the resistivity decreases with temperature as for degenerate semiconductors and residual resistivity ratios around 3–5 and mobility values up to $70 \text{ cm}^2/\text{V s}$ at room temperature are measured. Since the carrier concentration slightly decreases when lowering the temperature, the Hall mobility, defined as the ratio between Hall coefficient and resistivity, increases at low temperature reaching a value of about $400 \text{ cm}^2/\text{V s}$ at 10 K.

The mobility can also be independently evaluated by magnetoresistivity data according to the classical theory of

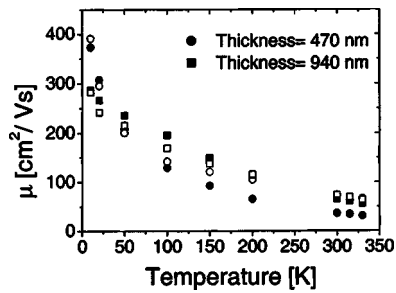


FIG. 3. Mobility as a function of the temperature for 470 and 940-nm-thick films grown by a two-step deposition. The relaxation layers are 70- and 140-nm-thick, respectively. Hall mobility (closed symbols) and mobility estimated from magnetoresistivity data (open symbols) show an exponential decay with the temperature.

cyclotron orbits. The magnetoresistivity of a semiconductor $\Delta\rho/\rho_B = (\rho(B=0) - \rho(B))/\rho(B)$ in the limit $\Delta\rho/\rho_B \ll 1$ is quadratic in the magnetic field B and can be expressed as

$$\frac{\Delta\rho}{\rho_B} = A\mu^2 B^2, \quad (1)$$

where μ is the mobility and A is a numerical coefficient which depends on the scattering mechanism, being 2.15 for ionized impurity scattering and 0.38 for acoustic phonon scattering.²⁸ For ZnO, the impurity scattering case is assumed, with the Debye temperature of this compound being nearly 870 K,²⁹ much larger than our measuring temperatures.

In Fig. 3 the Hall mobility as a function of the temperature is reported for two samples with different thickness, together with the mobility evaluated by magnetoresistivity measurements. As one can see, the two sets of data fairly agree but at high temperature where the mobility extracted from magnetoresistivity exceeds the Hall mobility.

Summarizing, we deposit epitaxial zinc oxide thin films on (110) strontium titanate substrates, proving the possibility of integrating wurzite-type with perovskite-type structures. In order to obtain thin films with high structural and morphological quality together with high carrier mobility values, a thin ZnO buffer layer deposited at low temperature is introduced. Hall mobility values of about 70 cm²/V s are measured at room temperature; the mobility exponentially increases in metallic samples lowering the temperature up to 400 cm²/V s at 10 K.

The integration of a transparent semiconductor like ZnO with the fascinating class of perovskites opens the way to the fabrication of new devices with novel functionalities useful both for application and for fundamental studies.

The authors thank M. Canepa and L. Mattera for providing the spectroscopic ellipsometer and for useful discussion

on ZnO optical spectra. Financial support from CARIGE Foundation is also acknowledged.

- ¹J. A. Sans, A. Segura, M. Mollar, and B. Mari, *Thin Solid Films* **453-454**, 251 (2004).
- ²S. Masuda, K. Kitamura, Y. Okumura, S. Miyatake, H. Tabata, and T. Kawai, *J. Appl. Phys.* **93**, 1624 (2003).
- ³R. L. Hoffman, B. J. Norris, and J. F. Wager, *Appl. Phys. Lett.* **82**, 733 (2003).
- ⁴H. S. Bae, M. H. Yoon, J. H. Kim, and S. Im, *Appl. Phys. Lett.* **83**, 5313 (2003).
- ⁵E. S. Shim, H. S. Kang, J. S. Kang, J. H. Kim, and S. Y. Lee, *Appl. Surf. Sci.* **186**, 474 (2002).
- ⁶H. Kim, J. S. Horwitz, S. B. Qadri, and D. B. Chrisey, *Thin Solid Films* **420**, 107 (2002).
- ⁷J. N. Zeng, J. K. Low, Z. M. Ren, T. Liew, and Y. F. Lu, *Appl. Surf. Sci.* **197**, 362, (2002).
- ⁸R. D. Vispute, V. Talyansky, Z. Trajanovic, S. Choopun, M. Downes, R. P. Sharma, T. Venkatesan, M. C. Woods, R. T. Lareau, K. A. Jones, and A. A. Iliadis, *Appl. Phys. Lett.* **70**, 2735 (1997).
- ⁹E. M. Kaidashev, M. Lorenz, H. von Wenckstern, A. Rahm, H. C. Semmelhack, K. H. Han, G. Benndorf, C. Bundesmann, H. Hochmuth, and M. Grundmann, *Appl. Phys. Lett.* **82**, 3901 (2003).
- ¹⁰H. Tampo, A. Yamada, P. Fons, H. Shibata, K. Matsubara, K. Iwata, and S. Niki, *Appl. Phys. Lett.* **84**, 4412 (2004).
- ¹¹M. Sugiura, Y. Nakashima, T. Nakasaka, and T. Kobayashi, *Appl. Surf. Sci.* **197**, 472 (2002).
- ¹²A. Tiwari, C. Jin, D. Kumar, and J. Narayan, *Appl. Phys. Lett.* **83**, 1773 (2003).
- ¹³T. Shimizu and H. Okushi., *J. Appl. Phys.* **85**, 7244 (1999).
- ¹⁴T. Kudo, M. Tachiki, T. Kashiwai, and T. Kobayashi, *Jpn. J. Appl. Phys., Part 2* **37**, L999 (1998).
- ¹⁵M. Sugiura, K. Uragou, M. Tachiki, and T. Kobayashi, *J. Appl. Phys.* **90**, 187 (2001).
- ¹⁶H. Katsu, H. Tanaka, and T. Kawai, *J. Appl. Phys.* **90**, 4578 (2001).
- ¹⁷Y. Watanabe and M. Okano, *Appl. Phys. Lett.* **78**, 1906 (2001).
- ¹⁸P. Fons, K. Iwata, S. Niki, A. Yamada, K. Matsubara, and M. Watanabe, *J. Cryst. Growth* **209**, 532 (2000).
- ¹⁹R. A. M. Azzam and N. M. Bashara, *Ellipsometry and Polarized Light* (North-Holland, Amsterdam, 1977).
- ²⁰C. M. Herzinger and B. D. Johs, U.S. Patent No. 5 796 983, 1998.
- ²¹S. Zollner, A. A. Demkov, R. Liu, P. L. Fejes, R. B. Gregory, P. Alluri, J. A. Curless, Z. Yu, J. Ramdani, R. Droopad, T. E. Tiwald, J. N. Hilfiker, and J. A. Woollam, *J. Vac. Sci. Technol. B* **18**, 2242 (2000).
- ²²G. E. Jellison, L. A. Boatner, D. H. Lowndes, R. A. McKee, and M. Godbole, *Appl. Opt.* **33**, 6053 (1994).
- ²³G. E. Jellison, Jr. and L. A. Boatner, *Phys. Rev. B* **58**, 3586 (1998).
- ²⁴K. Postava, H. Sueki, M. Aoyama, T. Yamaguchi, Ch. Ino, Y. Igasaki, and M. Horie, *J. Appl. Phys.* **87**, 7820 (2000).
- ²⁵R. Bel Hadj Tahar and N. Bel Hadj Tahar, *J. Appl. Phys.* **92**, 4498 (2002).
- ²⁶C. Agashe, O. Kluth, J. Hupkes, U. Zastrow, B. Reck, and M. Wuttig, *J. Appl. Phys.* **95**, 1911 (2004).
- ²⁷M. Lorentz, E. M. Kaidashev, H. von Wenckstern, V. Riede, C. Bundesmann, D. Spemann, G. Benndorf, H. Hochmuth, A. Rahm, H. C. Semmelhack, and M. Grundmann, *Solid-State Electron.* **47**, 2205 (2003).
- ²⁸K. Seeger, *Semiconductor Physics*, Springer Series in Solid State Sciences (Springer, New York, 1997), 6th ed.
- ²⁹T. I. Nedoseikina, A. T. Shuvaev, and V. G. Vlasenko, *J. Phys.: Condens. Matter* **12**, 2877 (2000).